Investigating small RPAS ground impact injury severity criteria (phase 1 report)

Weng, Yuhu; Bian, Kewei; Gunasekaran, Kalish; Gholipour, Javad; Vidal, Charles; Mao, Haojie; National Research Council Canada. Aerospace Research Centre

https://doi.org/10.4224/40002733

Investigating small RPAS Ground Impact Injury Severity Criteria
Phase 1 Report

Yuhu Weng[1], Kewei Bian[1], Kalish Gunasekaran[1], Javad Gholipour[2], Charles Vidal[2] and Haojie Mao[1, 3]

1 Mechanical and Materials Engineering, Faculty of Engineering, Western University, London, Ontario, Canada

2 National Research Council, National Research Council Canada – Aerospace Research Center

2107 Chemin de la Polytechnique, Montréal Québec, Canada H3T 1J4

3 School of Biomedical Engineering, Western University, London, Ontario, Canada

Abstract
The project was focused on investigating sRPAS to human head impact safety. A finite element (FE) model of a representative quadcopter sRPAS was developed. The FE sRPAS model impacted average adult male model and head kinematics data were predicted. The model predictions were validated against cadaveric data.

Based on validated computational simulations, various injury metrics including HIC (head injury criteria), BrIC (brain injury criteria), peak head linear accelerations, and peak rotational velocity were analyzed. A strong correlation between HIC15 and peak linear acceleration was observed. Also, BrIC strongly correlated with peak rotational velocity. Minimizing the structural effect of the quadcopter sRPAS, HIC15 was found to positively correlate with skull stresses. BrIC was found to be moderately correlated with brain strains evaluated using cumulative strain damage measure (CSDM).

Sensitivity analysis on impact location and impact angle revealed that head kinematics would be affected by slight changes of impact location and impact angle.

Head kinematics, HIC, BrIC, skull stress, and brain strain were compared between average male and small female using computational simulations. Small female head experienced almost twice of HIC and 40% more BrIC as average female head experienced.

Keywords: sRPAS, UAS, Drone, Impact, Safety, Finite Element, Skull stress, Brain strain

1. Problem Statement and Background

With the technological innovations in small RPAS (remotely piloted aircraft system), also referred to as small UAS (unmanned aircraft system), sRPAS has been widely used for commercial, recreational and personal purposes (1). The market of sRPAS was evaluated as $609 million in 2014 and is expected to quickly grow to $4.8 billion in 2021 (2). There is an elevated level of risk involving RPAS operations near and over people. Hence, research into improving sRPAS safety is urgently needed.

The project was designed to support the development of injury criteria for sRPAS to people on the ground impacts. The critical pre-existing knowledge is based on the field's understanding of human head injury and Alliance for System Safety of UAS through Research Excellence (ASSURE) #14 report, in which cadaveric experiments, dummy experiments, and computational simulations of small RPAS to body impacts have been documented. After reviewing existing research, two major gaps were identified.

1) Understanding how a variety of populations such as average male and small female respond differently during sRPAS to head impacts.
2) Understanding how existing head injury criteria, such as head injury criterion (HIC), can be used to regulate drone safety.

Established THUMS ver. 4.02 average male and small female human body models were chosen as these THUMS models have been extensively validated in terms of skull force, brain motion,

brain pressure, and neck responses. Moreover, ver. 4.02 models carry the detailed brain for brain strain predictions. While both the average male and small female THUMS models were calibrated by the same developer, the cadaveric data specified for small female head-neck system was not adopted for small female model validation. **Hence, the majority of this study (Sections 2, 3 and 4) was conducted using the average male model, while the investigation of small female model response was reported in Section 5 to promote the protection of vulnerable population.**

2. Development and Validation of a Representative Quadcopter sRPAS Model

Method of model development and validation

Details of available cadaver data, model development, and validation methods are described in this section.

Available cadaver data for validation

The drone to human collision cadaver test data are available through ASSURE reports (3). The Post-Mortem Human Surrogate (PMHS) experiments were conducted by the Ohio State University. Overall, 41 sRPAS to human head collision tests were conducted, in which 17 quadcopter-sRPAS-related experimental data could be used for validation with detailed time histories. In the 17 experiments, 3 different cadaver subjects were involved, and all the subjects were males with body masses of 170 lbs (77.1 kg), 164 lbs (74.4 kg) and 143 lbs (64.9 kg), respectively. The experiments were conducted at different angles and locations, including 4 typical location settings as frontal 58 degree, lateral 0 degree, lateral 58 degree and top 90 degree. All PMHS subjects were instrumented with head kinematics sensors to measure head linear acceleration, head rotation velocity and head rotation acceleration at head center gravity during impacts.

sRPAS model

A representative quadcopter sRPAS finite element (FE) model (**Figure 1**) was developed by using HyperMesh (Altair, Troy, MI USA). The model was divided into various parts and meshed separately, including body shell upper portion, body shell lower portion, motor casing, motor, camera assembly fixture, camera, circuit board, battery support and battery. Totally, the FE quadcopter sRPAS model contains 43,863 elements, including 14,673 3D hexahedral elements, 45 3D prism elements, 29055 2D quads elements, 82 2D triangular elements and 8 1D beam element. The mesh quality for the FE model was meticulously improved to a high level. For 3D solid elements, only 1.0% of elements had warpage greater than 5 with the maximum value of 13.39. All 3D elements had aspect ratio below 5 with maximum aspect ratio of 3.38. 2.6% of elements had Jacobian less than 0.7 with the minimum value of 0.56. 1.6% of elements had element length less than 1 mm with the minimum value of 0.7 mm. 3.8% of elements had element length greater than 3.5 mm with the maximum value of 4 mm. For 2D shell elements, 4% of elements had warpage value greater than 5 with the maximum value of 15.01. All 2D elements had aspect ratio below 5 with the maximum value of 4.16. 1.8% of 2D elements had Jacobian value smaller than 0.7 with the minimum value of 0.44. All 2D elements had element length greater than 1mm and 6.5% elements had length greater than 3.5 mm with maximum length of 4.98 mm.

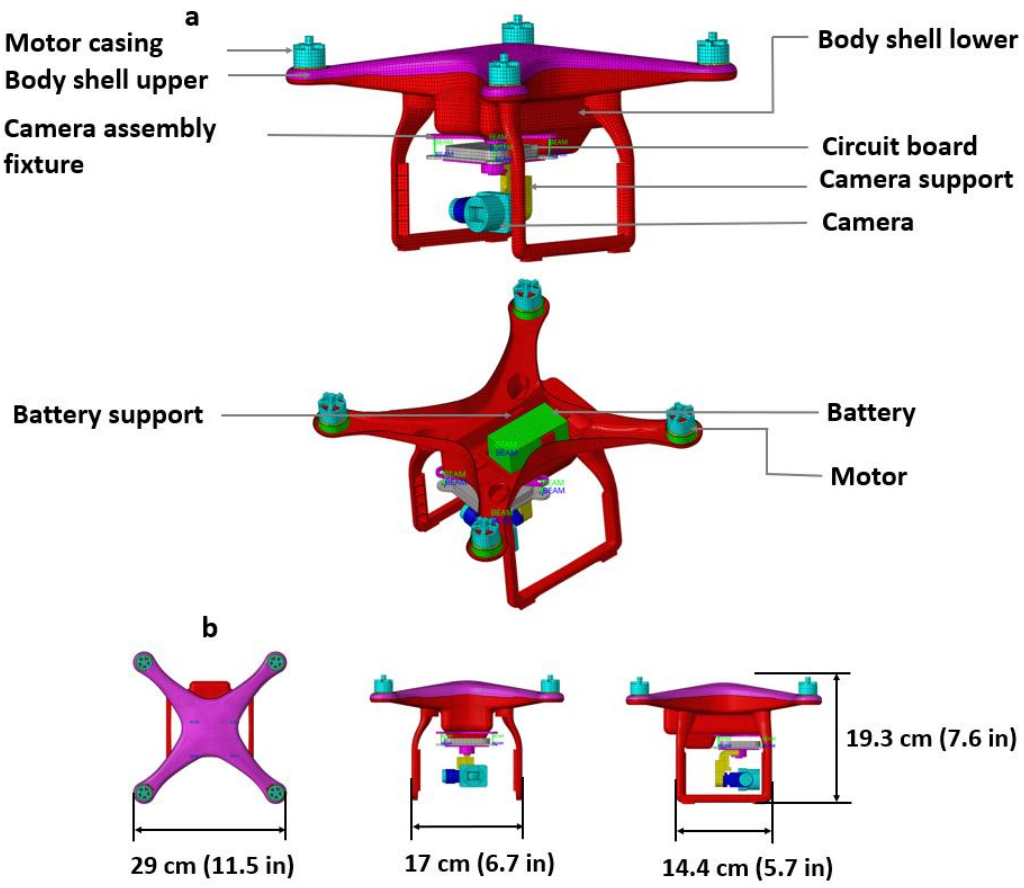

Figure 1 sRPAS finite element model

The sRPAS FE model was defined with the upper and bottom body shells being separated. For a physical sRPAS object, the upper and bottom body shells were connected by clips located at the shell edge. During the collision, these weakly connected clips would break, and the upper and lower body shells would separate due to shell deformation. While for the arm portion, screws were used to reinforce the connection between two shells, preventing separation. To better represent this feature in the FE model, the node connections between upper and bottom shell were implemented at four drone arms and there was no node connection in the rest of edge space (**Figure 2**). Due to deformation, force would transfer between the upper and bottom shells through the edge between them. Therefore, edge-to edge contact was added in the FE model.

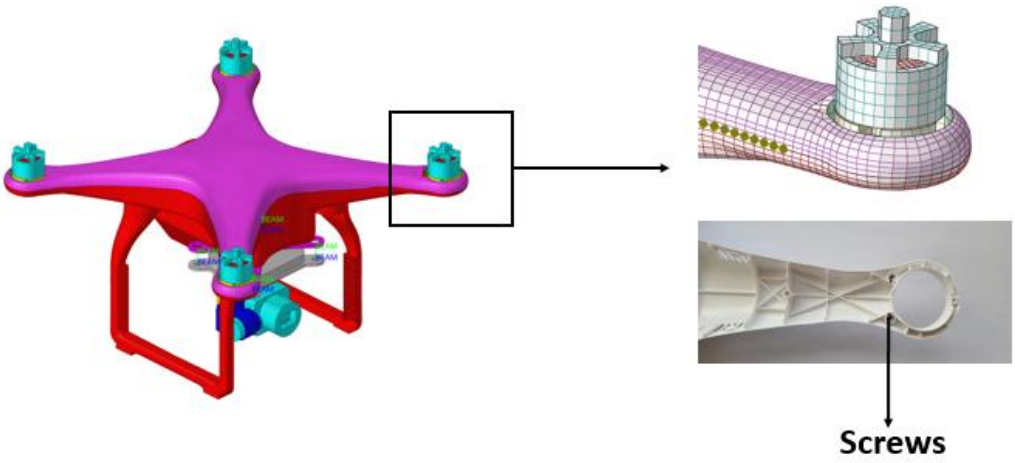

Figure 2 Drone upper and bottom shell connections

The body shell thickness was one major factor affecting the overall sRPAS stiffness. To determine the thickness of body shell, 10 different locations were selected and measured by a Vernier caliper on both upper and bottom drone shell. The measurements yielded an average of 1.34 mm with a standard deviation of 0.094 mm. In addition, on body shell, there were strengthened bars which would increase stiffness. By both measuring the average drone body shell thickness and considering the effect of strengthened bars, the final thickness of body shell was defined as 1.5 mm.

The material properties of various parts of the sRPAS FE model were referred to published data in ASSURE #A14 report and are summarized in **Table 1**. **Table 1**a shows materials of each specific part. The most critical materials which could have potentially affect simulation results were presented in the FE model. Polycarbonate was assigned to the body shell and camera supporter. The camera assembly fixture, camera, and motor casing were defined using Cast Aluminum 520F. Motor was defined using Steel 4030. The circuit board was defined using G10 Fiber glass. The battery and battery support was simplified as elastic materials. The FE model has a total weight of 1.207 kilograms, which is consistent with the physical model. **Table 1**b shows the drone material properties.

The body shells were the most critical parts during collisions because the shells would directly contact with human head. The energy of a moving sRPAS would first transfer from body shells to head. Therefore, the material property of drone body shell was estimated to play an important role of sRPAS to human collision. In general, the shell was made from polycarbonate plastic which was a strong and tough material used in engineering structures. According to ASSURE report, Johnson-Cook model was found appropriate to simulate polycarbonate plastic, because it can better present material elastic and plastic deformation during collision. **Table 1**c summarizes the material properties of polycarbonate.

Table 1 Material properties
a Parts and material types

Drone Part	Material
Drone body shell	Polycarbonate
Camera assembly fixture	Cast Aluminum 520 F
Camera	Cast Aluminum 520 F
Motor casing	Cast Aluminum 520 F
Motor	Steel 4030
Circuit board	G10 Fiber glass
Camera supporter	Polycarbonate
Battery support	Elastic
Battery	Elastic

b General material properties

Material	Young's modulus (MPa)	Poisson's ratio	Density (ton/mm^3)
Cast Aluminum 520F	66,600	0.33	2.87E-09
Steel 4030	200,500	0.29	8.65E-09
G10 Fiber glass	13,790	0.12	1.98E-09
Elastic	500	0.33	5.477E-09

c Detailed material properties of polycarbonate

Density (kg/m^3)	Young's Modulus (GPa)	Shear Modulus (GPa)	A (MPa)	B (MPa)	C	m	n	Cv (KJ/kgK)	Tmelt (K)
1197.8	2.59	0.93	80	75	0.0052	0.548	2	1.3	562

THUMS version 4.02 male model

The Total Human Model for Safety (THUMS) version 4.02 50 percentile male model was used as a primary tool to investigate drone-to-human collision head responses. This model was developed and released by Toyota Motor Corporation. For the version 4.02, the models can simulate internal organ injuries at tissue level. The head model of this version has very detailed head parts, including the skin, skull, facial bones, eyeballs, meninges, cerebrum, cerebellum, brainstem, and cerebrospinal fluid (CSF). Especially, Version 4.02 models have very detailed brain meshes and the element length of the brain part was around 1.2 to 5 mm. The version 4.02 male model contains 772,156 nodes and 1,975,599 elements with a total mass of 77.6 kilograms. The head model was validated by several experiments, including translational impact conducted by Nahum et al. (1977) to validate brain pressures (**Figure 3**a); translational impact conducted by Yoganandan et al. (1995) to validate skull impact forces (**Figure 3**b); translational and rotational impact conducted by Hardy et al. (2001) and Kleiven and Hardy (2002) to validate brain-skull relative motion (**Figure 3**c). The neck parts of THUMS model was validated by dynamic axial loading experiments conducted by Nightingale et al. (1997) (**Figure 3**d).

Beside the 50 percentile male model, the 5 percentile female model was also used as reported in **Section 5** to promote protection of vulnerable populations. It needs to be acknowledge that validation against small female cadaveric head-neck data has yet to be conducted.

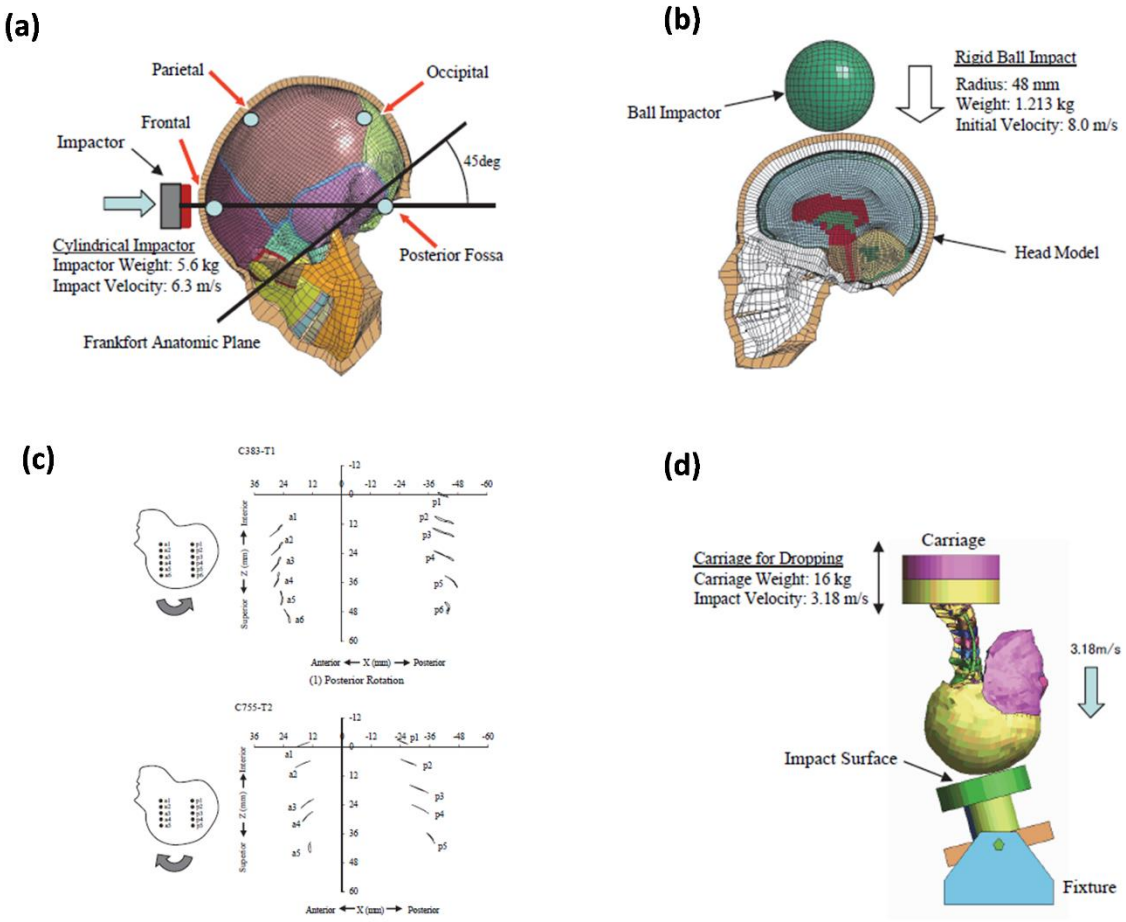

Figure 3 THUMS head and neck model validations (from THUMS manual)

sRPAS to head impact

Simulation of DJI Phantom 3 to human head impact

Both Hypermesh and LS-PrePost version 4.3 (LSTC/ANSYS, Livermore, CA) was used for sRPAS model and human body model integration, initial condition setups including adjusting sRPAS position relative to human head, setting sRPAS flying velocity, and defining contact condition between sRPAS and human head. The initial position, angles and velocities were referred to OSU PMHS experiments settings (**Table 2**) as reported in ASSURE report (3). **Figure 4** shows the 50 percentile THUMS model (**Figure 4**a) and four typical sRPAS-to-head impact directions, including lateral 0 degree (**Figure 4**b), frontal 58 degree (**Figure 4**c), lateral 58 degree (**Figure 4**d) and top 90 degree (**Figure 4**e). The INITIAL_VELOCITY in LS-DYNA (LSTC/ANSYS, Livermore CA) was used to assign the flying velocity. The AUTOMATIC_SURFACE_TO_SURFACE was used to define the contact between sRPAS

model and human head model. The friction coefficient was set as 0.3. The numerical accelerometers were defined on the human head model to collect linear acceleration and rotation velocity at head center of gravity.

***Table 2 sRPAS to head impact setups*. FPS: foot per second. OSU: Ohio State University.**

Case #	Impact Direction	Impact Angle (Degree)	Gender	Impact Velocity (m/s - FPS)	Cadaver test case #	Cadaver Subject #
1	Right side	0	Male	16.8 - 55.1	OSU #2	1
2	Right side	0	Male	18.3 - 60.1	OSU #3	1
3	Right side	0	Male	21.1 - 69.2	OSU #4	1
4	Front	58	Male	17.5 - 57.3	OSU #6	1
5	Front	58	Male	18.0 - 59.2	OSU #8	2
6	Front	58	Male	18.3 - 59.9	OSU #8a	2
7	Front	58	Male	21.4 - 70.1	OSU #9	2
8	Right side	58	Male	18.7 - 61.2	OSU #10	2
9	Right side	58	Male	21.9 - 71.9	OSU #11a	2
10	Top	90	Male	16.8 - 55.2	OSU #13	2
11	Top	90	Male	19.5 - 63.9	OSU #14	2
12	Top	90	Male	21.5 - 70.5	OSU #15	2
13	Right side	58	Male	18.6 - 60.9	OSU #16a	3
14	Right side	58	Male	21.9 - 72	OSU #17	3
15	Front	58	Male	21.9 - 71.8	OSU #19	3
16	Top	90	Male	19.7 - 64.5	OSU #22	3
17	Top	90	Male	21.5 - 70.5	OSU #23	3

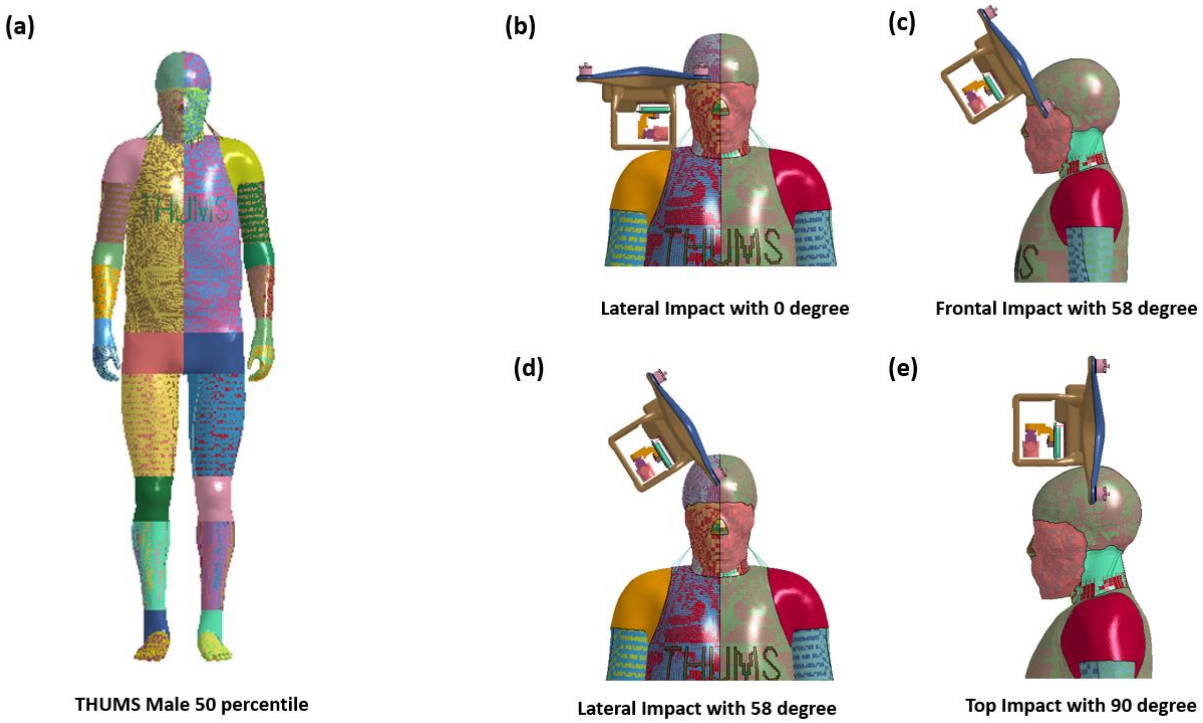

Figure 4 THUMS version 4.02 50% male model (a) & typical impact directions (b-e)

Results of Model Development and Validation

All the simulations were calculated using LS-DYNA. Computers with Intel Xeon 8-core CPUs and 24-core CPUs was used to solve simulations. When using 2 CPUs, it took approximately 20 hours to solve 40-millisecond impact cases.

The results in this section are for THUMS male model.

Linear acceleration

Under lateral 0 degree impact (cases 1, 2 and 3, **Figure 5**), typically one peak linear acceleration appeared during the impact. The durations of the impact were approximately 2 milliseconds. The curve shape and impact duration matched well for all three cases. The simulated peak linear acceleration also matched with cadaver experiments, except for case 3 in which a high initial velocity (71 FPS) was defined. For case 3, the peak linear acceleration of simulation was about 20% smaller than that of the experiment details provide by ASSURE.

In frontal 58 degree cases with drone close to face cases (case 4, 5, 6 and 7), the linear acceleration curves typically had 2 peaks and the second peak was generally similar to or lower than the first peak. The impact duration was around 3 milliseconds. Except case 5, the curve shape and peak linear acceleration matched well with cadaver experiments. In case 5, the simulation curve did not match with experiment curve. However, the cadaver experiment curve of case 5 was not consistent with other three frontal 58 degree cases, showing three peaks with the last peak being the largest.

In lateral 58 degree cases (case 8, 9, 13 and 14), generally the simulation impact duration and curve shape matched well with cadaver experiments. However, in some cases the peak values were over predicted. In case 9 and 13, the peak linear accelerations were 17% and 35% higher than cadaver experiments. In case 14, the simulated peak value and curve shapes were close to the cadaver experiments.

Case 15 was a typical case in which the initial position of drone was close to coronal suture instead of the face. Under this case, the simulation and cadaver had similar peak linear accelerations, which were 370.9 g's and 378.2 g's, respectively. The impact durations were perfectly matched, which were around 2 milliseconds.

In top 90 degree cases (case 10, 11, 12, 16, and 17), the impact durations of cadaver experiments were roughly 1 millisecond longer than those of simulations. In general, the peak linear accelerations of cadaver experiments were larger than those of simulations, especially for the cases using cadaver subject 2 (case 10, 11 and 12). Under these three cases, the cadaver experiments had two peaks which were different from simulations where only one peak appeared. Under cases using cadaver subject 3 (case 16, 17), the model-predicted peak linear accelerations were close to cadaver results and the curve shapes were very similar. From average linear acceleration bar charts of all 17 cases, we can observe that average peak linear accelerations of simulation was 4.5% lower than that of experiment.

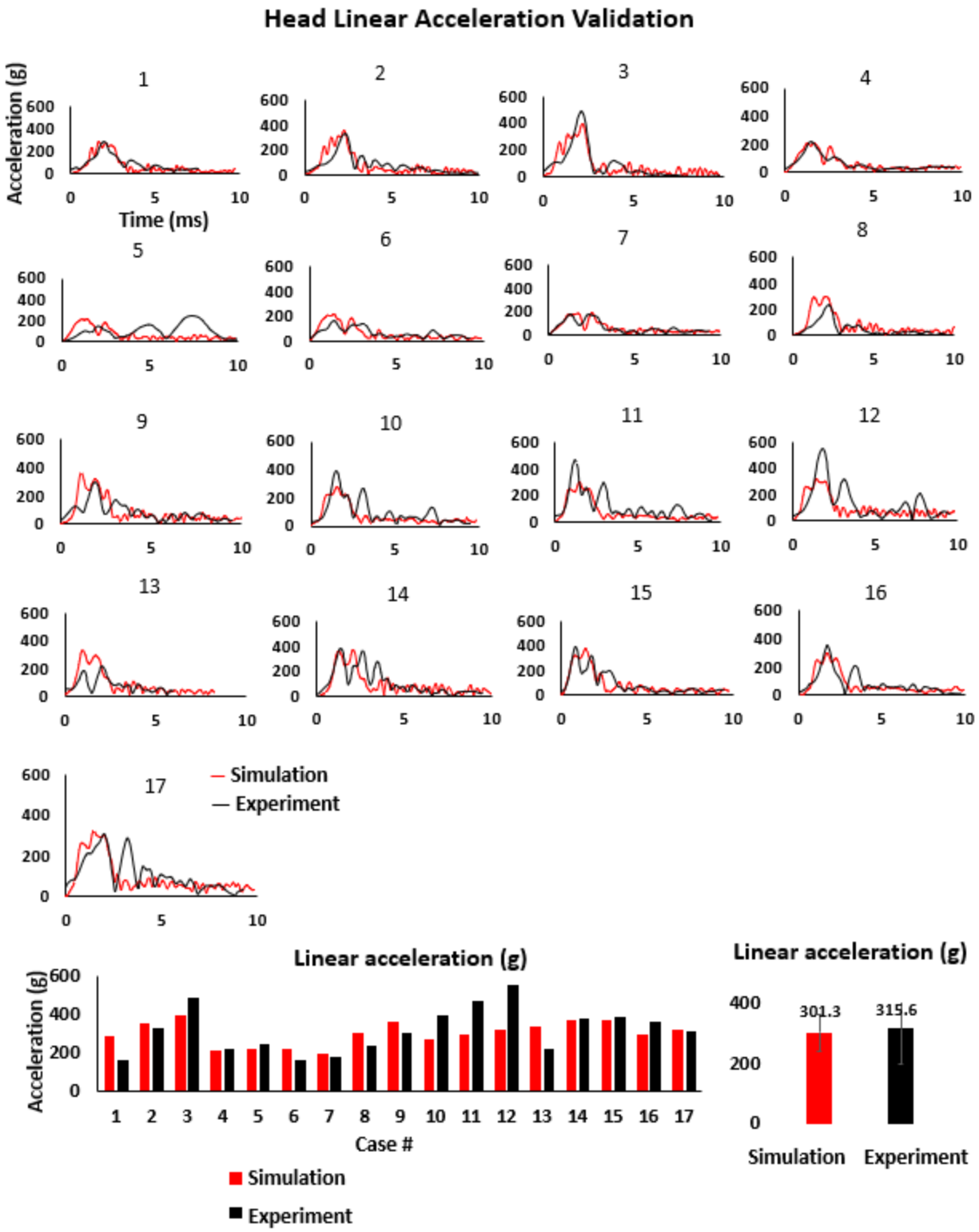

Figure 5 Head linear acceleration validation. Red curves and bars indicate simulation data while black curves and bars indicate experimental data.

Rotational velocity

In lateral 0 degree cases (case 1, 2 and 3, **Figure 6**), the rotation velocity curves were well validated. The curves of simulations and cadaver experiments matched well, and the peak rotation velocity values were generally close.

In frontal 58 degree cases (case 4, 5, 6, and 7), the curve shapes and trends matched well. However, under low initial velocity (case 4, 5 and 6 which had initial velocity of 56, 61 and 61 FPS, respectively), the simulated peak rotation velocity values were under predicted by approximately 50%. However, under high velocity (case 7 with initial velocity of 71 FPS), the peak value and curve shape were well matched.

In lateral 58 degree cases (case 8, 9, 13 and 14), generally the peak rotation velocities were overpredicted. In case 8 and case 13, the peak rotation velocity values were overpredicted by 29% and 14%, respectively. In case 13 and 14, the curve shape and trend were matched. However, the peak values were 29% and 24% higher than those of experiments.

In frontal 58 degree with initial drone position closing with coronal suture case (case 15), the simulation and experiments curves had different shapes. However, the peak rotation velocity values were close, which were 1410 degree/second and 1443 degree/second, respectively.

In top 90 degree cases (case 10, 11, 12, 16 and 17), the curve shapes were similar. Generally, the peak rotation velocity of simulation were underpredicted. In case 10 and 11, the simulated peak rotation velocities were 17% and 18% lower than experimental results. In case 12, the predicted peak value was 11 % higher than that of experiment. In case 16 and 17, the peak rotation velocity values were 19% and 29% lower than experimental results. From average bar charts of rotation velocity, the average peak rotation velocity was 2% lower than that of experiment.

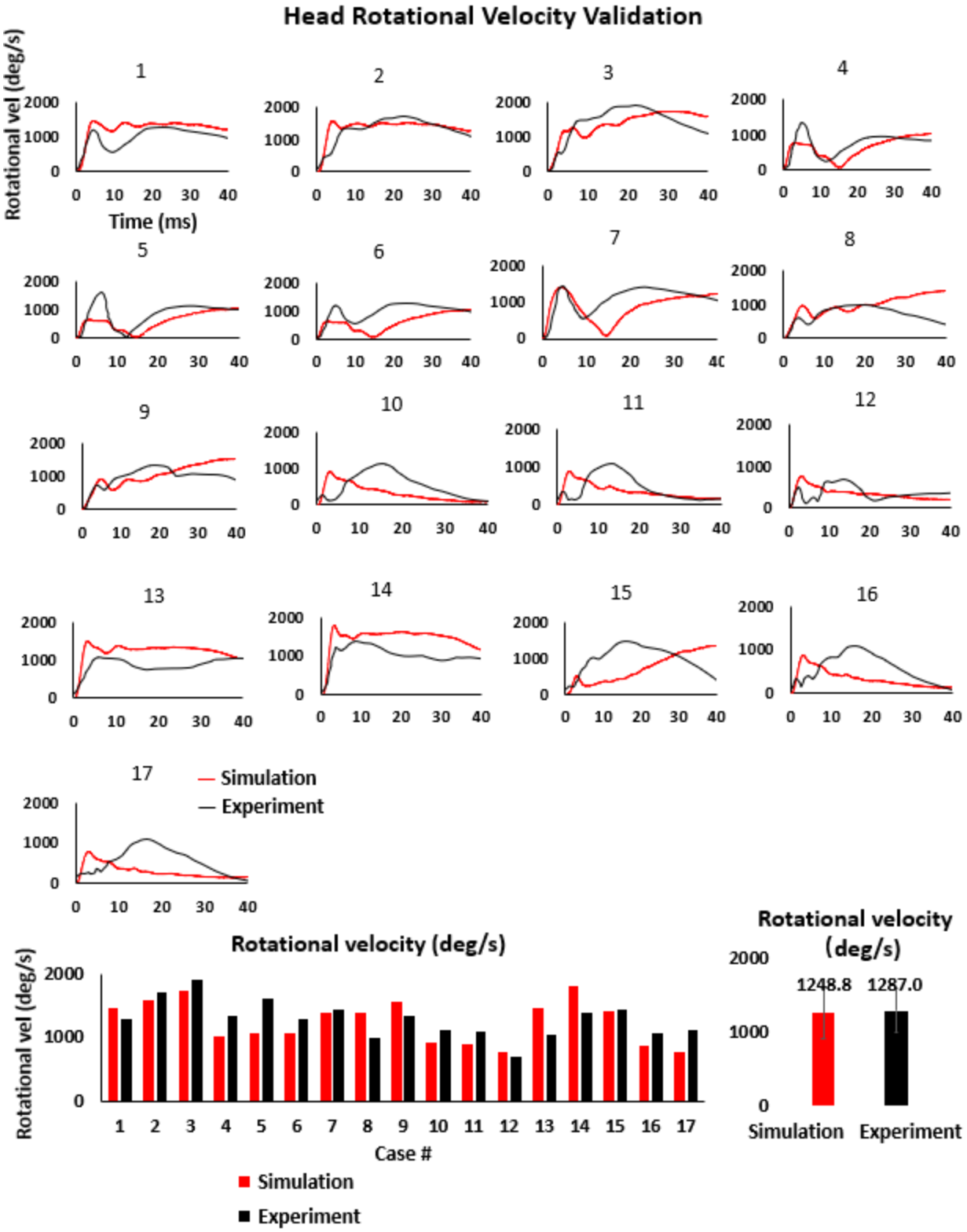

Figure 6 Head rotation velocity validation. Red curves and bars indicate simulation data while black curves and bars indicate experimental data.

3. Injury metric analysis

Head injury criterion (HIC)

Head injury criterion (HIC) is accepted in automotive safety. It can be calculated using the equation below. Generally the data is collected from the accelerometer mounted at the center of gravity of the head.

$$HIC = \max_{t_1, t_2} \left\{ (t_2 - t_1) \left[\frac{1}{t_2 - t_1} \int_{t_1}^{t_2} a(t) dt \right]^{2.5} \right\}$$

where t1 and t2 are the initial and final times of the maximum HIC interval and a(t) is the measured acceleration of head center gravity. t2 – t1 is constrained to 15 ms when calculating HIC15, and the time interval (t2 – t1) that yields the maximum HIC value will be equal to or smaller than 15 ms.

To calculate HIC of each impact case, the numerical accelerometer was defined at the location of head center of gravity to collect linear acceleration data. The linear accelerations at x, y, and z directions were outputted every 0.01 millisecond (100K frequency). The original output data were then filtered by low-pass filter using CFC 1000 HZ. MATLAB 2019 was then applied to calculate the resultant linear acceleration using the filtered x, y, and z data. An in-house code was written to calculate HIC15. In needs to be noted that for sRPAS to human head collision, the impact durations were relatively short (1 to 3 milliseconds), and the maximum HIC values were realized at a duration (t2 – t1) of less than 3 milliseconds. The commonly used HIC15 could be continuously used.

Brain injury criteria (BrIC)

Brain injury criteria is a relatively newly developed injury metric to assess brain injury caused by the rotational motion of head. The mathematical formulation is expressed below:

$$BrIC = \sqrt{\left(\frac{\omega_x}{\omega_{xC}}\right)^2 + \left(\frac{\omega_y}{\omega_{yC}}\right)^2 + \left(\frac{\omega_z}{\omega_{zC}}\right)^2}$$

Where ω_x, ω_y, and ω_z are maximum angular velocities in X, Y, and Z-axes, respectively. ω_{xC}, ω_{yC}, and ω_{zC} are the critical angular velocities in their respective directions.

In this study, the maximum angular velocities at x, y, z direction were collected from head center of gravity. The rotation velocity data were filtered by CFC 180 HZ. According to the literature, the critical angular velocity applied at x, y and z directions were 66.25, 56.45 and 42.87 rad/s (average of CSDM and MPS based) respectively (4).

Maximum skull stress

The maximum skull stress was obtained from LS-PrePost version 4.03. Normally, the maximum skull stress happened at very beginning of collision. In LS-PrePost, all the solid parts of trabecular

bones were temporally masked, and only head skull shells were represented (**Figure 7a**). The von Mises (VM) stress was checked at the contact location between sRPAS and human head (**Figure 7b**). To better represent the maximum skull stress value of the contact area, an average strategy was applied. The time histories of VM stress of nine different elements, which were visually selected based on stress contours, were plotted and the averaged curve was obtained (**Figure 7c& d**). The maximum value on the averaged curve represented as the maximum skull stress.

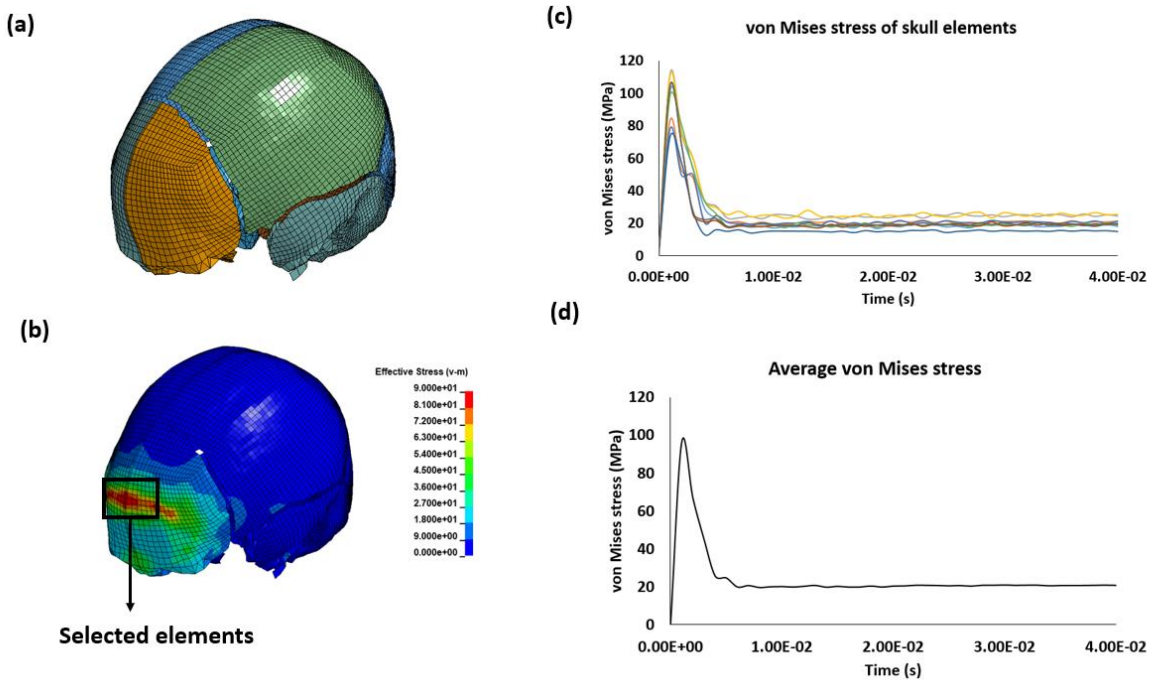

Figure 7 Maximum skull stress collection

Cumulative strain damage measure (CSDM)

The CSDM is a method to evaluate the deformation-related brain injuries caused by head impact. It can be calculated by the fraction of brain experiencing strain level greater than various specified level. In this study, the volume of all the elements which experienced a strain level over specified threshold values was recorded and the fraction of recorded volume to the total brain volume would be the CSDM value. For CSDM10 and CSDM15, the volume of brain elements experiencing strains above 0.1 and 0.15 would be calculated. The calculated CSDM values were further verified with brain strain contour to confirm a visual agreement between high CSDM and large high-strain areas.

Results of Injury Metrics

Table 3 shows all the results collected from 17 cases, including peak linear acceleration, peak rotation velocity, HIC, BrIC, maximum skull stress, CSDM10 and CSDM15.

Table 3 Head kinematics & Injury metrics results

Case #	Peak Linear acceleration (g)	Peak rotation velocity (deg/s)	HIC	BrIC	Maximum skull stress	CSDM10	CSDM15
1	284	1467	1311	0.428	71.0	0.638	0.251
2	354	1581	1800	0.464	77.6	0.686	0.329
3	391	1730	2380	0.490	83.9	0.571	0.151
4	213	1017	690	0.315	102.0	0.503	0.074
5	220	1075	757	0.334	100.0	0.486	0.069
6	218	1067	749	0.332	104.0	0.458	0.059
7	194	1393	543	0.431	107.0	0.824	0.493
8	304	1398	1669	0.407	62.3	0.240	0.015
9	364	1556	2074	0.445	76.3	0.230	0.012
10	272	931	1138	0.288	26.5	0.143	0.016
11	298	897	1481	0.278	25.8	0.132	0.015
12	317	777	1957	0.242	66.7	0.064	0.001
13	337	1473	1652	0.405	72.6	0.584	0.191
14	371	1812	2233	0.510	86.8	0.728	0.361
15	371	1409	2124	0.439	127	0.256	0.028
16	295	865	1482	0.268	25.6	0.111	0.013
17	321	780	1987	0.242	65.8	0.066	0.008

HIC, linear acceleration, and skull stress

In general, there was a strong correlation between HIC and peak linear acceleration with R squared value of 0.9474 (**Figure 8**). Putting all 17 cases together (with different impact direction and angles), HIC did not have strong correlation with maximum skull stress (**Figure 9a**). Excluding all frontal cases, it was observed that HIC and skull stress had moderate level of correlation with R squared value of 0.5426 (**Figure 9b**). Under only top 90 cases for which structural variances were minimized, HIC and skull stress had strong correlation with R squared value of 0.8356 (**Figure 9c**). Under lateral cases including 0 degree and 58 degree allowing some structural influences, the R squared value was 0.5923 (**Figure 9d**).

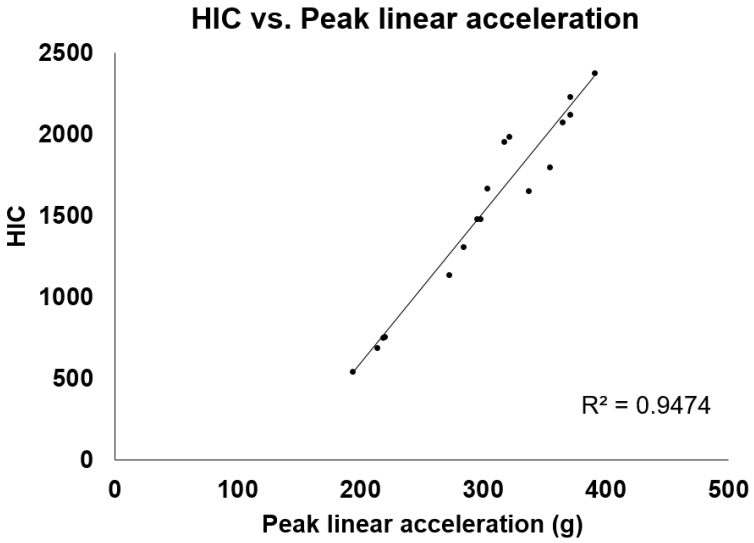

Figure 8 Correlation between HIC and Peak linear acceleration

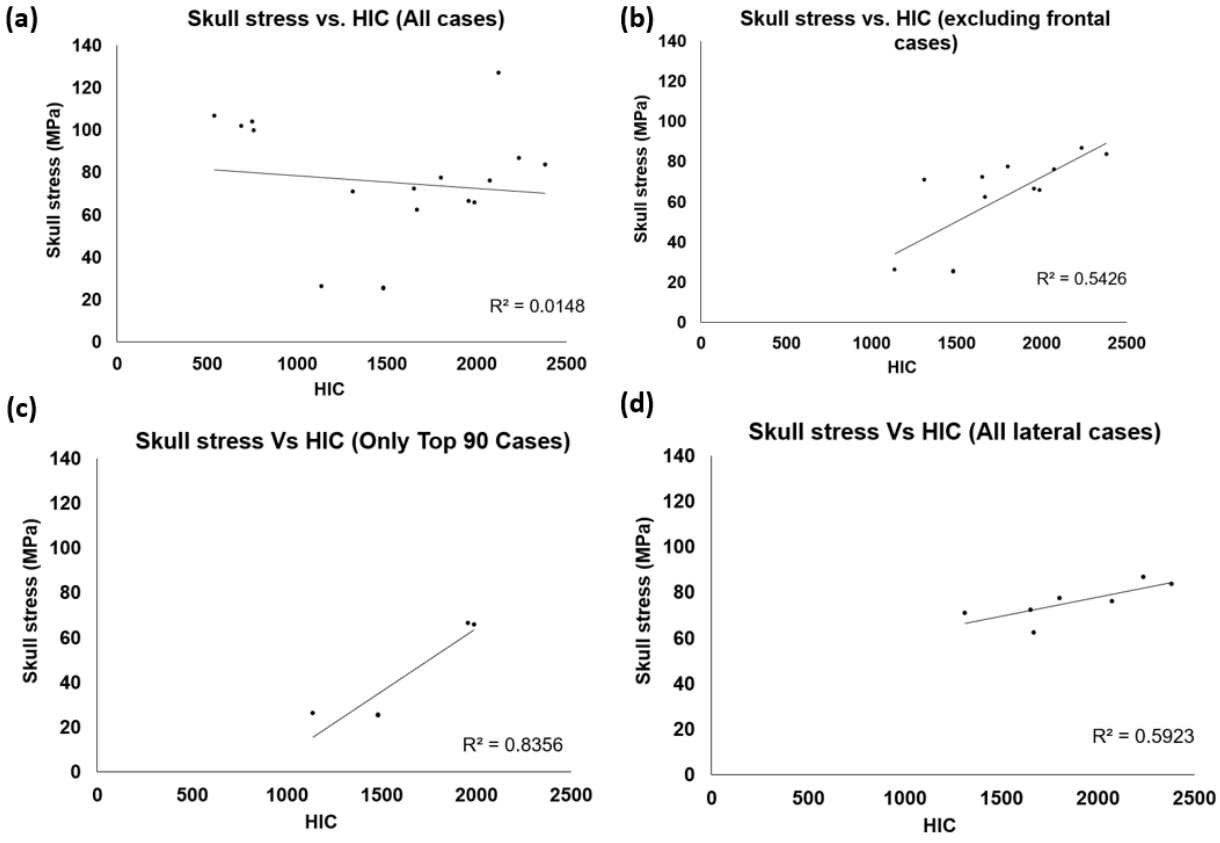

Figure 9 Correlations between HIC and maximum skull stress

Variances in skull stresses (**Figure 10**) further demonstrate the effect of sRPAS structures. For example, while top 90 degree impacts have similar impact velocities as other impacts (**Table 2**), the skull stresses were much lower than those in other cases due to relatively larger contact areas.

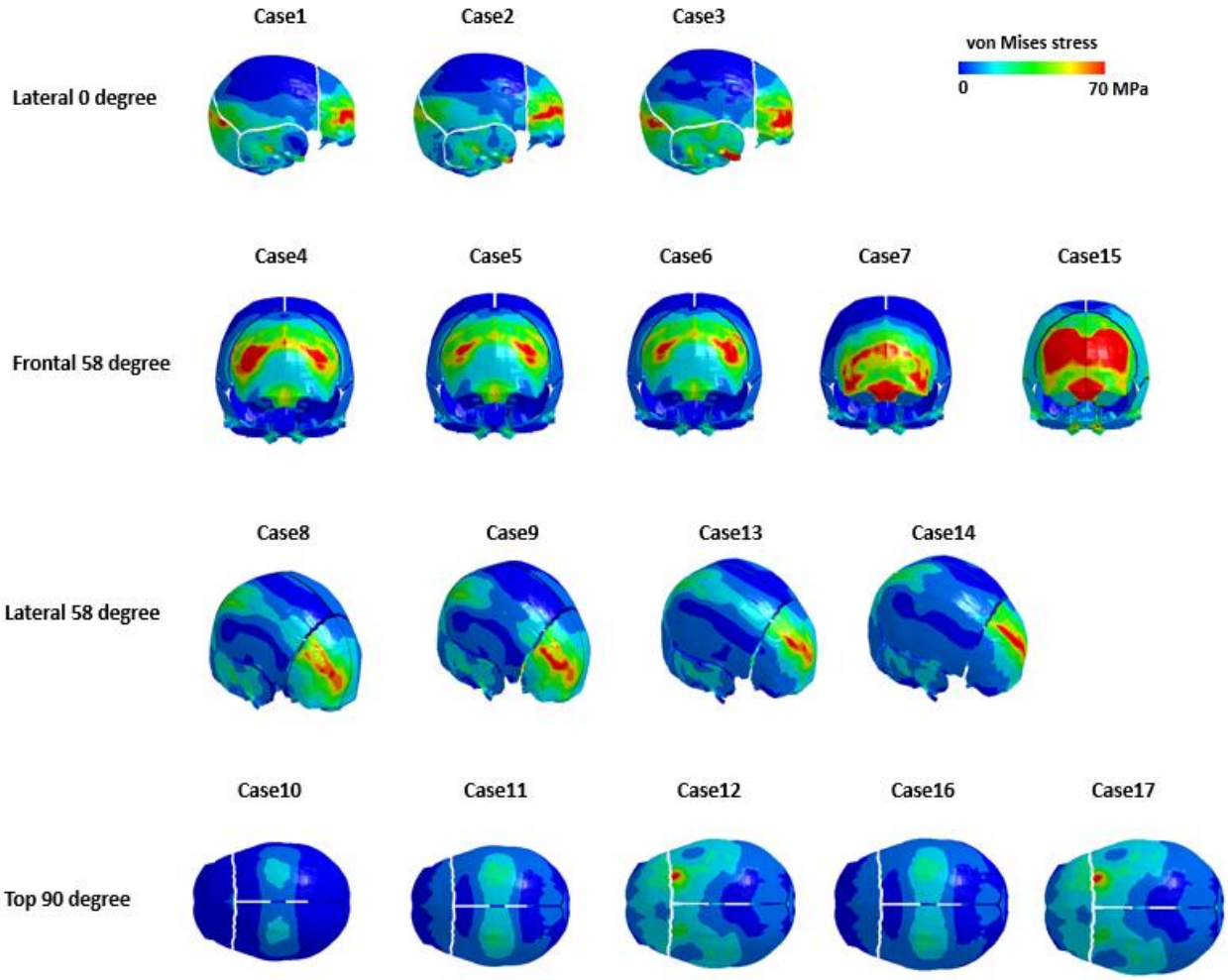

Figure 10 Skull stress contours

BrIC, rotational velocity, and brain strain

The BrIC and rotation velocity had strong correlation with R squared value of 0.9825 (**Figure 11**). For all 17 cases, it was observed that CSDM10 and CSDM15 had some correlation with peak rotation velocity with R squared values of 0.4923 and 0.379 (**Figure 12a**). The BrIC and CSDM had some correlation with R squared value of 0.519 (**Figure 12b& c**). The BrIC had lower correlation with CSDM15 than CSDM10 (**Figure 12d**).

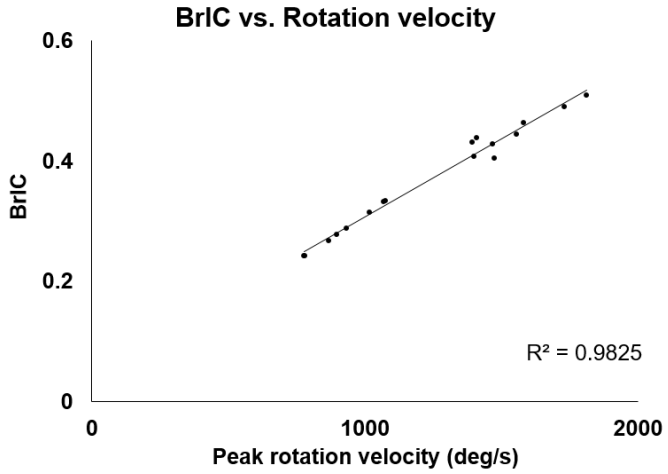

Figure 11 Correlation between BrIC and rotation velocity

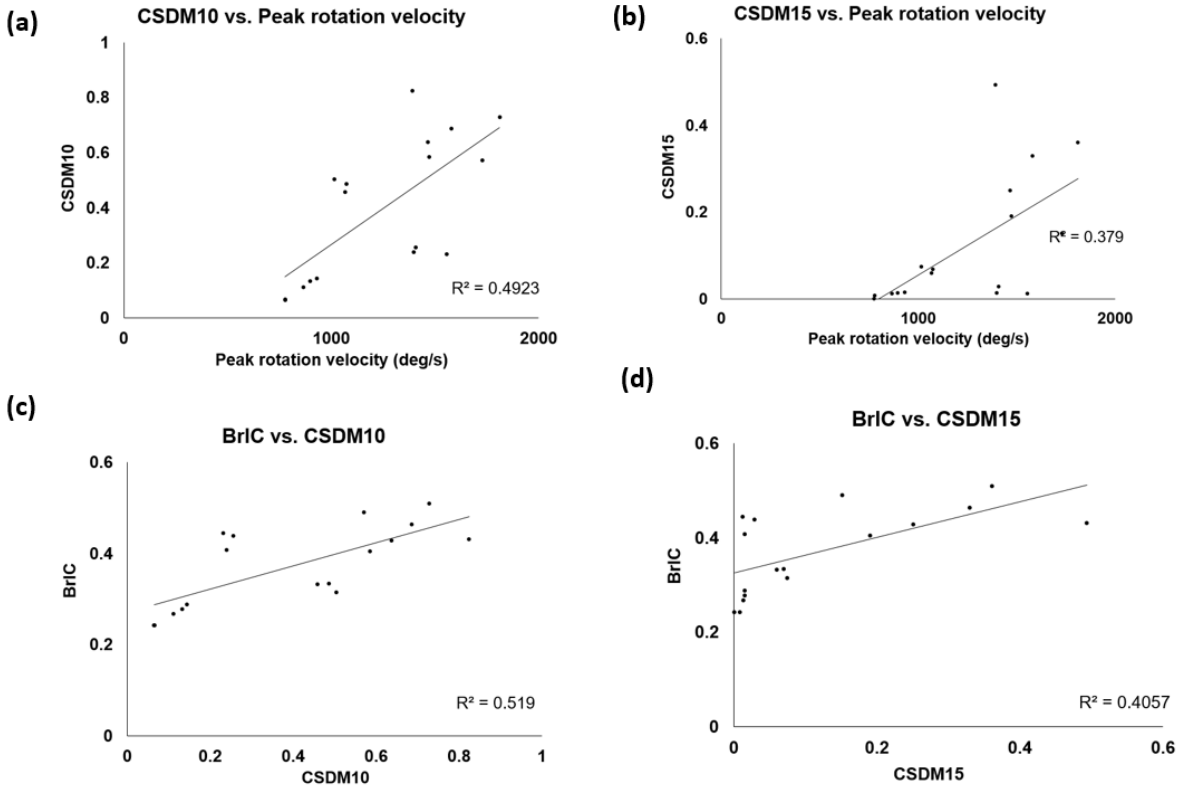

Figure 12 Correlations between CSDM and peak rotation velocity

Brain strain

Brain contour (**Figure 13**) demonstrates that relatively high brain strains were produced for several situations (such as cases #1, 2, 3, 7, 13, and 14), while in other cases especially top 90 degree impacts the strains were small.

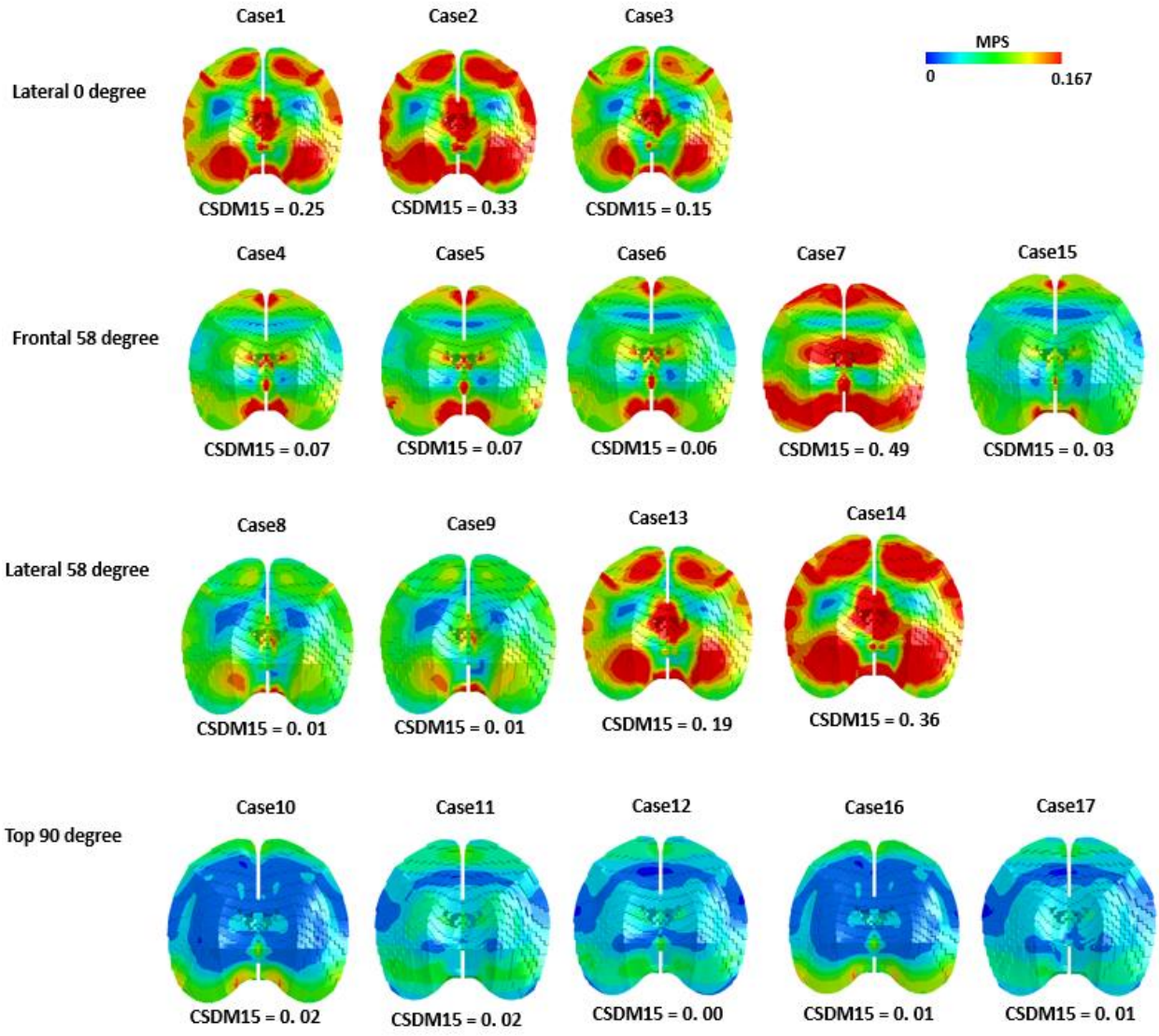

Figure 13 Brain strain contours

4. Sensitivity Analysis

Impact location and angle

In setting up impact conditions, it was found that it was hard to perfectly sure about the exact impact angles and impact locations of experiments. Also, it could be reasonably postulated three cadaver heads used in experiments possessed different shapes that could further affect the

definition of impact location and angle. Hence, despite the FE model has been exercised to best match with experimental settings, a sensitivity analysis on the impact location and angle could help to understand the changes of head kinematics due to such changes. Four typical direction cases (**Figure 14**) were used as original cases for sensitivity study. For angle sensitivity of all directions, the impact angles were increased and decreased at 3 degrees, which was consistent with the parametric setting in the ASSURE report. For impact position sensitivity, the initial positions were changed at 5 mm and 10 mm perpendicular to the moving direction of sRPAS, which were based on our estimates. All other variables were kept the same as baseline cases.

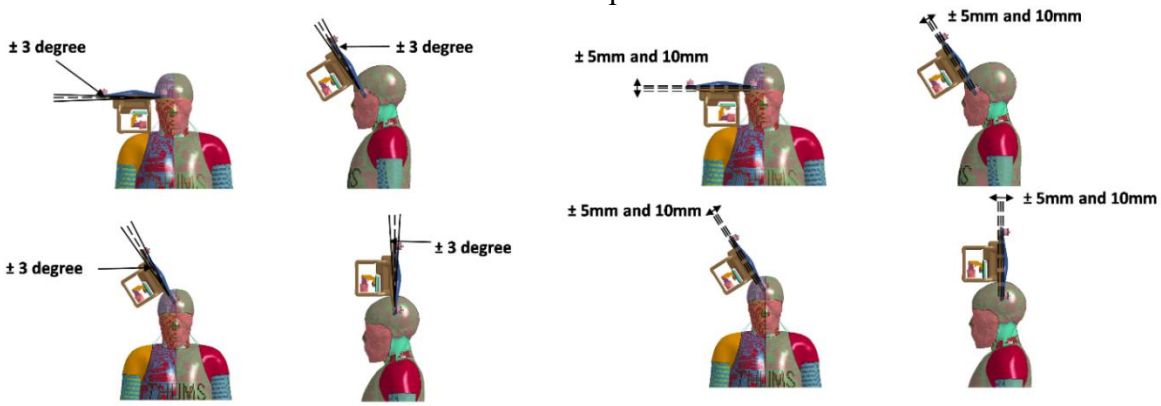

Figure 14 Simulation setups of sensitivity study

Results - The effect of impact angle

From peak linear acceleration bar chart (**Figure 15**), in general it can be observed that, with the increase of angle, the head linear acceleration had an increase trend and the changes depended on the impact directions. In minus 3 degree cases, under lateral impact cases (0 degree and 58 degree), the peak linear acceleration increased. For frontal and top cases, the peak value decreased. Under top 90 degree impacts, with 3 degree angle change cases, the peak linear acceleration had around 30% of variation.

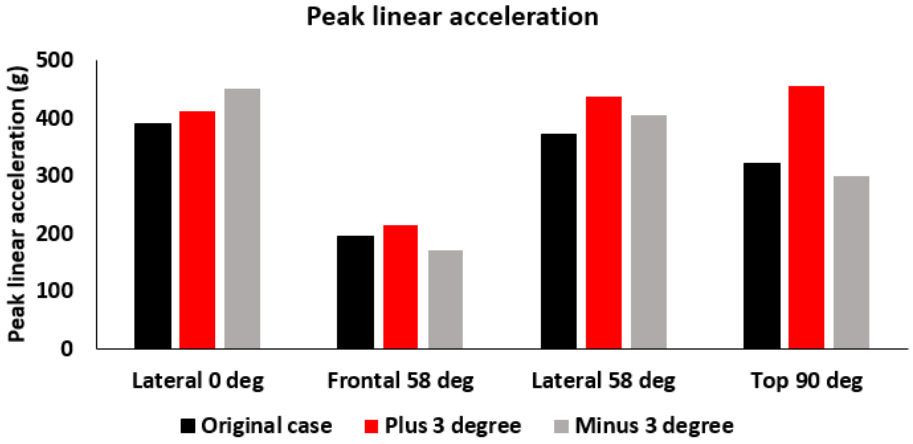

Figure 15 Peak linear acceleration of angle adjustments

In peak rotation velocity chart (**Figure 16**), in general the variation was relatively small. However, it can be observed the largest variance also happened in top 90 degree cases which had 29% of variations.

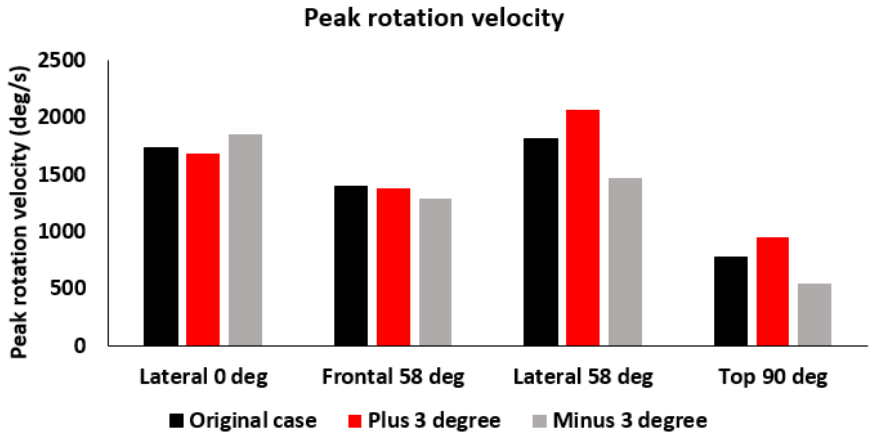

Figure 16 Peak rotation velocity of angle adjustments

Results - The effect of impact location

Figure 17 shows the head peak linear acceleration due to the change of impact location. It can be observed that under lateral 0 degree and frontal 58 degree impacts, the linear acceleration was not very sensitive to location changes with maximum variation of 19.5%. However, under lateral 58 degree and top 90 degree impacts, the location change had larger effect on head peak linear acceleration. Under those directions, 10-mm location change induced around 27.0% of variation.

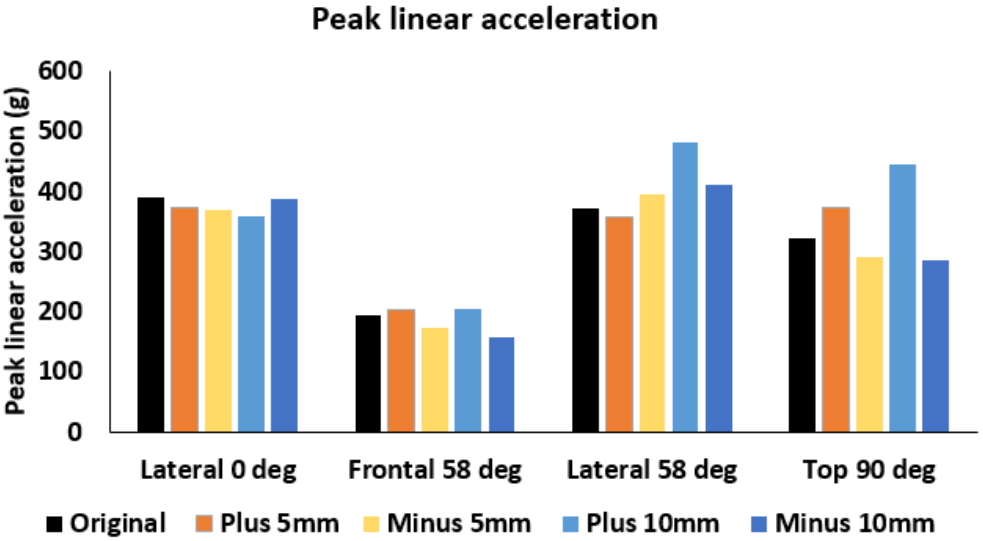

Figure 17 Peak linear accelerations under various impact locations

The effect of impact location change on peak rotation velocity (**Figure 18**) was generally similar as it had on peak linear acceleration. In lateral 0 degree and frontal 58 degree impacts, the head rotations did not change much due to impact location changes. In lateral 58 degree and top 90

degree impacts, head rotational velocities were more sensitive to location shift and showed a maximum variation of 21.9%.

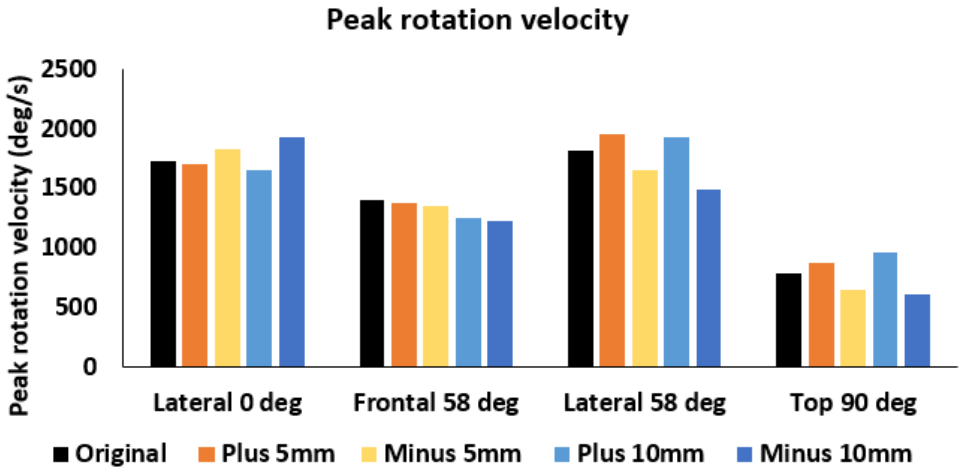

Figure 18 Peak rotation velocities under various impact locations

5. Average male vs. small female

THUMS version 4.02 female model

The Total Human Model for Safety (THUMS) version 4.02 5 percentile female model was used to investigate the head repsonses. **Figure 19** shows the comparsion of THUMS male and female model. It could be seen that the small female model overall was not simply a scaled down model (**Figure 19**a), while the head-neck portions between average male and small female were similar (**Figure 19**b). Same as the male model, the female model was generated by intergraiting component models (head, torso and extremity models). Totally, the model contains 2,514,045 elements and 878,461 nodes. The total weight of model is 49 kilograms and the height of the model is 153 cm. The head and neck models of THUMS female were also verified using the similar impact settings used for the male model. Meanwhile, it should be noted that the validation of small female model was based on the same group of cadaveric data instead of small-female-specific cadaveric data.

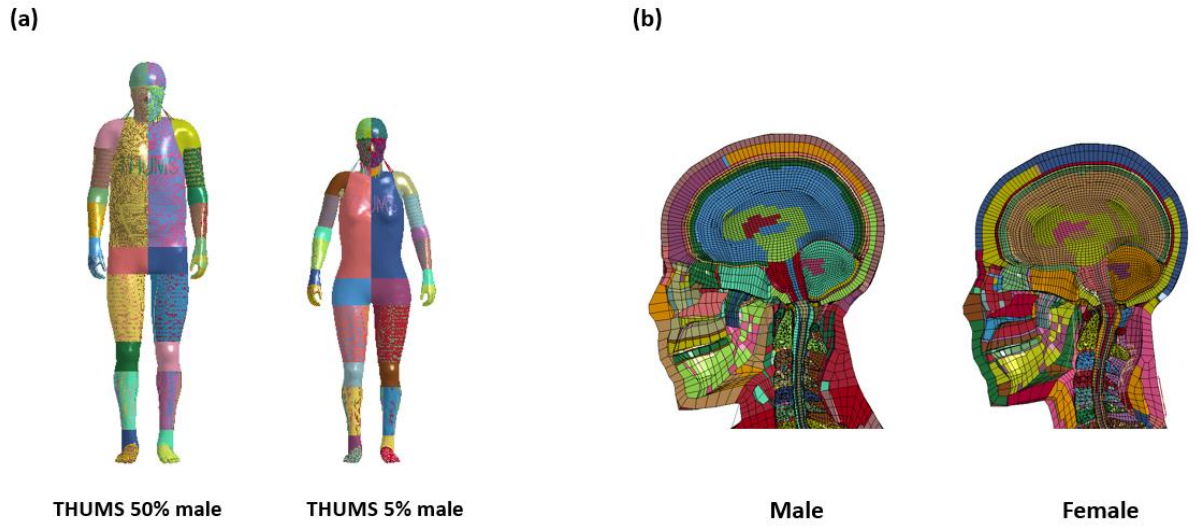

Figure 19 THUMS male and female model comparison

Impact settings

Similar as the male model, the female model was also installed with an accelerometer at head center of gravity to collect the head kinematics. Four typical sRPAS-to-head impact directions were used to setup the simulation (**Figure 20**). Overall, 17 simulations were conducted on female model. The detailed setup information can refer to **Table 2**. To ensure the impact locations were the same as those for male cases, a proportional method were applied. A vertical line through head center of gravity was selected as reference and the impact locations were determined by the angles between vertical center line and drone flying directions.

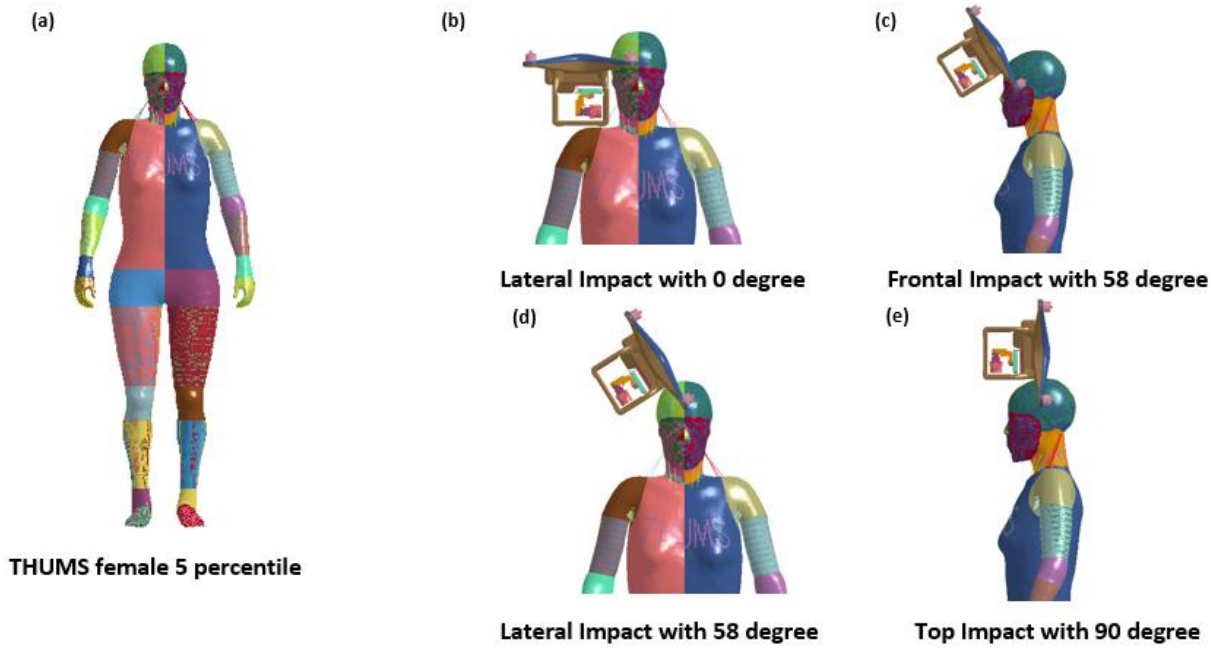

Figure 20 Typical impact directions

Resutls of comparing male to female

Table 4 summarizes the results collected from 17 female cases, including peak linear accelreation, peak rotation velocity, HIC, BrIC, maximum skull stress, CSDM10 and CSDM15.

Table 4 Female head kinematics and injury metrics results

Case #	Peak Linear acceleration (g)	Peak rotation velocity (deg/s)	HIC	BrIC	Maximum skull stress (MPa)	CSDM10	CSDM15
1	454	2328	3105	0.734	67.3	0.888	0.568
2	498	2599	3817	0.799	69.3	0.9209	0.632
3	556	2216	5488	0.724	79.8	0.901	0.591
4	282	1319	1459	0.410	97.0	0.685	0.208
5	291	1407	1611	0.437	97.6	0.725	0.266
6	284	1360	1538	0.424	98.1	0.712	0.247
7	254	2742	1169	0.849	65.7	0.956	0.757
8	395	1723	2961	0.627	74.4	0.660	0.153
9	443	1912	3638	0.680	99.8	0.734	0.244
10	331	1097	2053	0.340	29.0	0.114	0.015
11	336	1101	2550	0.342	28.9	0.120	0.017
12	355	992	2989	0.308	36.2	0.092	0.015
13	408	1784	2979	0.644	47.8	0.769	0.308
14	443	2509	4057	0.782	73.5	0.913	0.605
15	383	1755	3030	0.544	71.3	0.572	0.116
16	344	1111	2502	0.344	28.0	0.125	0.018
17	329	557	2301	0.176	28.7	0.064	0.009

Linear kinematics and skull stress

Generally, there was a strong correlation between HIC and peak linear acceleration with R sqaured value of 0.9204 (**Figure 21**a). Using all 17 cases to correlate skull stress and HIC, there was no correlation between them (**Figure 21**b). However, when the frontal cases were excluded, the skull stress and HIC showed certain level correaltion with R squarde value of 0.5895 (**Figure 21**c). Under all top 90 degree cases, the correlation of skull stress and HIC became higher with R square value of 0.6439 (**Figure 21**d).

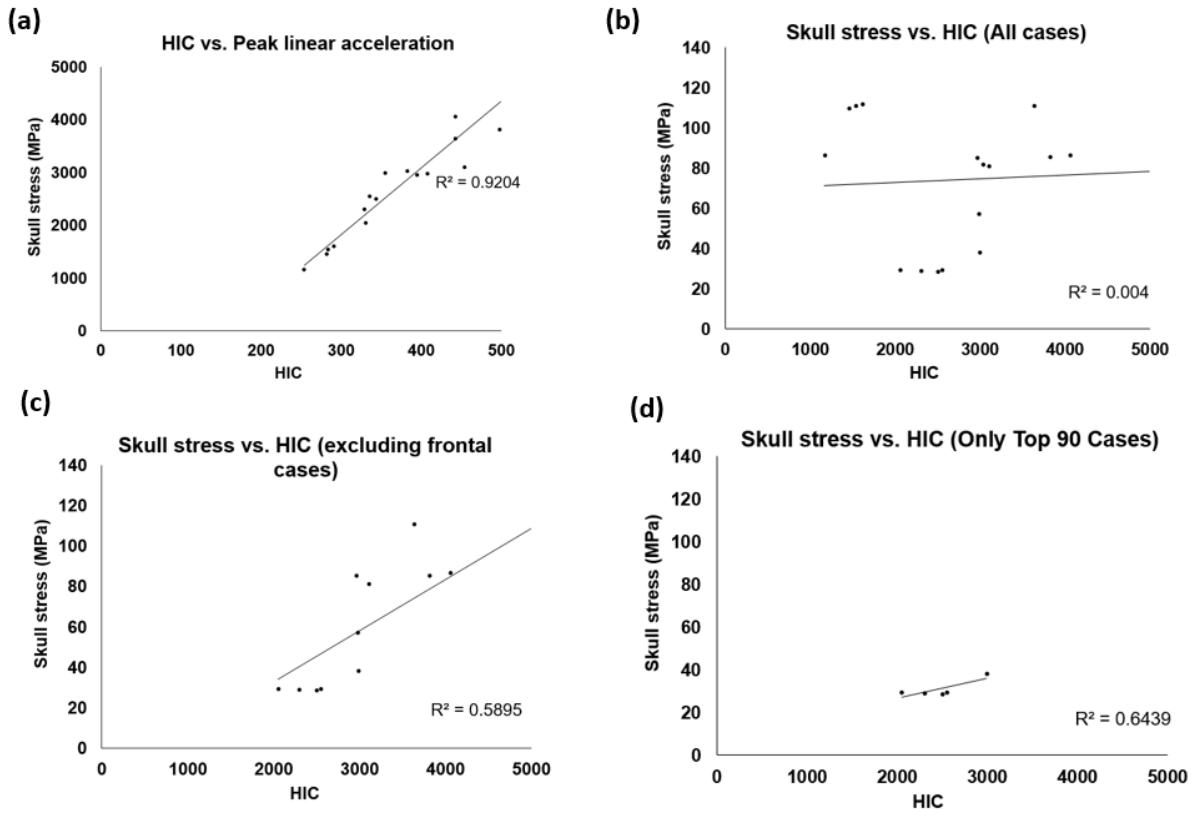

Figure 21 Correlation between HIC and peak linear acceleration & correlation between skull stress and HIC

Rotational kinematics and brain strain

The BrIC and rotation velocity had very strong correlation with R squares value of 0.9712 for female cases (**Figure 22**). It is observed that CSDM10 and CSDM15 had good correlation with peak rotation velocity with R square value of 0.768 and 0.864 respectively (**Figure 23a& b**). The BrIC and CSDM also had good correlations under female cases. For CSDM10 and CSDM15 with BrIC correlations, the R square value were 0.7851 and 0.7958, respectively (**Figure 23c& d**).

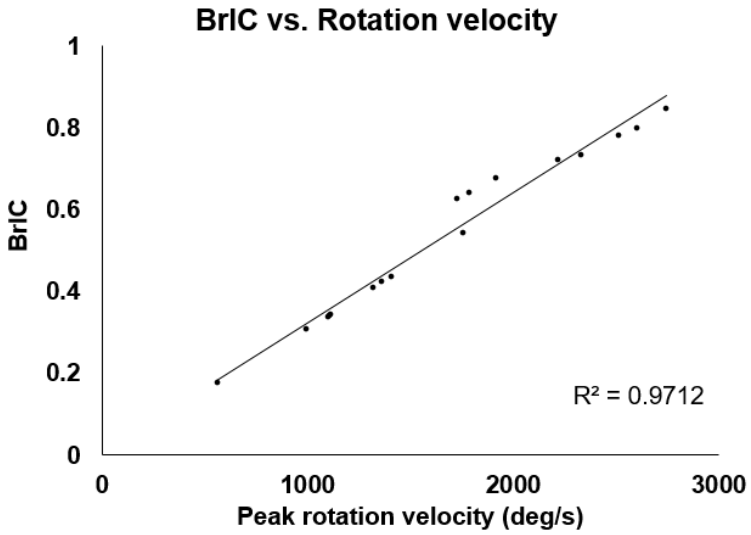

Figure 22 Correlation between BrIC and rotation velocity

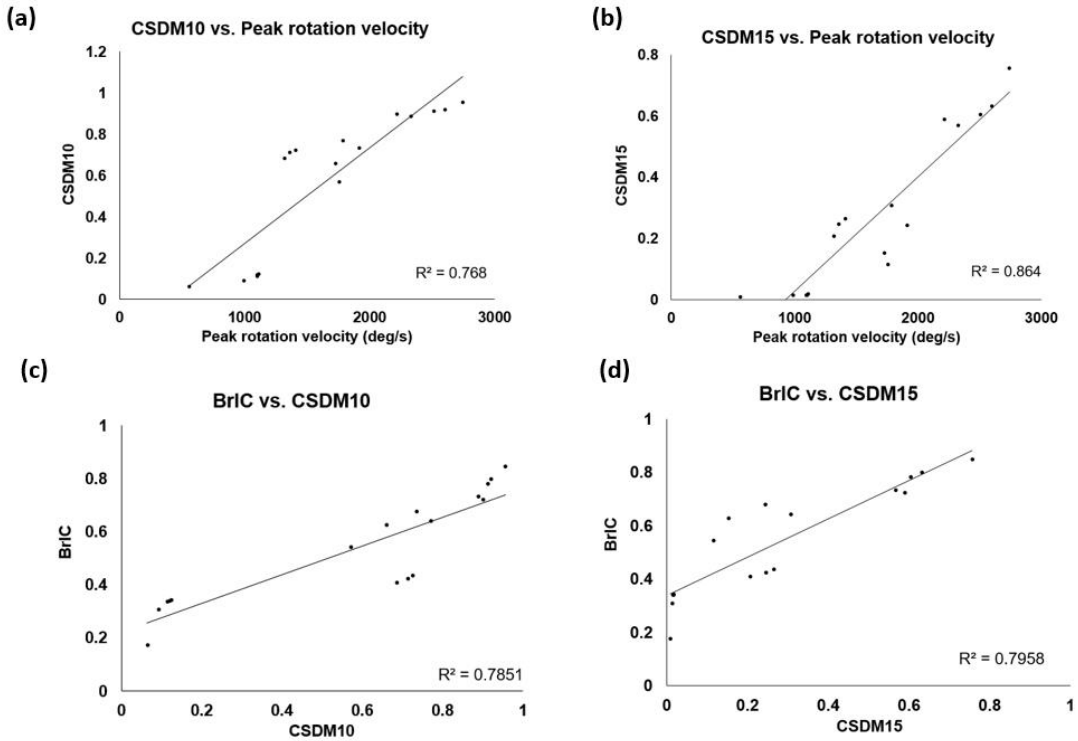

Figure 23 Correlation between CSDM and peak linear acceleration & Correlation between BrIC and CSDM

Average male vs. small female

Figure 24 shows the comparison of average value of all 17 cases. It was observed that small female suffered 25% higher averaged peak linear acceleration and 82% higher HIC than male (**Figure 24a& b**). However, under higher linear acceleration and HIC, female suffered similar average skull stress with male (**Figure 24c**).

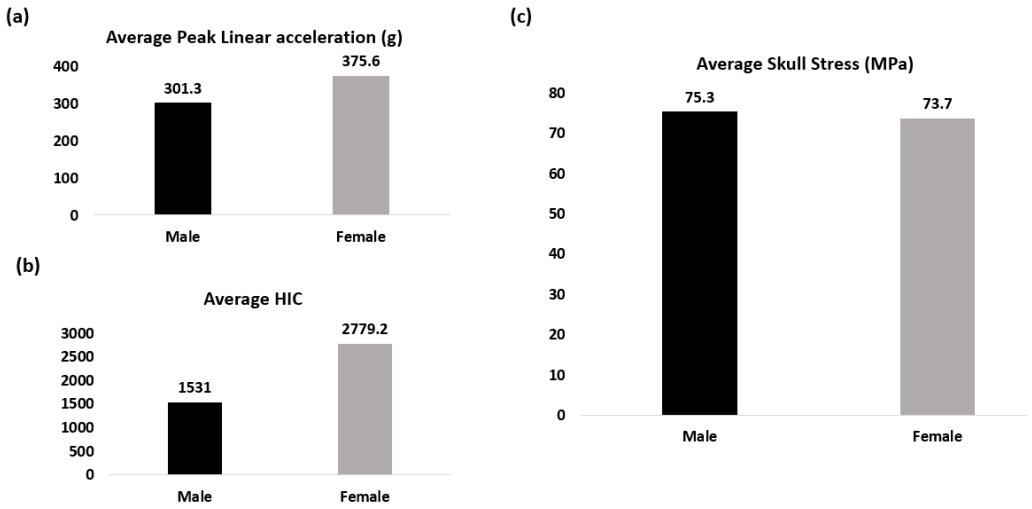

Figure 24 Average peak linear acceleration, HIC and skull stress comparisons of male and female model

Generally, female suffered higher 24% higher peak roation velocity than male (**Figure 25**a). Small female experienced 29% higher BrIC than that of male (**Figure 25b**). For CSDM, small female expereienced 30% and 53% higher CSDM10 and CSDM15 (**Figure 25c& d**).

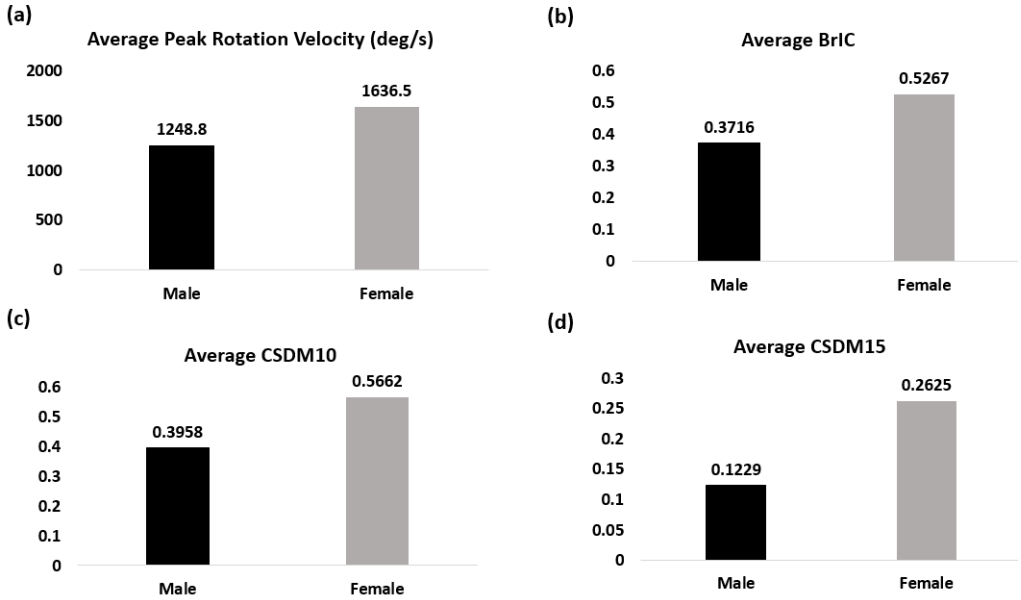

Figure 25 Average peak rotation velocity, BrIC and CSDM comparisons of male and female model

6. Injury risks

Using established AIS3+ risk curves (5), an average HIC15 of 1531 from male studies corresponds to >40% risk of AIS3+ head injuries. While an average HIC15 of 2779 from female head impacts corresponds to >70% risks of AIS3+ injuries.

The risk of AIS3+ brain injury based on BrIC was <10% for average male and <20% for small female. Compared to HIC15-related head injuries, these risk values are much lower.

7. Scalability

There is a weak correlation between kinetic energy and HIC with r squared value of 0.34 in the studied range of kinematic energy from 150 to 300 J (**Figure 26**). However, there is almost no correlation between kinetic energy and BrIC (**Figure 27**). The lack of correlation between kinetic energy with both HIC and BrIC was postulated due the structural effect, which highlighted the limitation of developing scalability using only one sRPAS model.

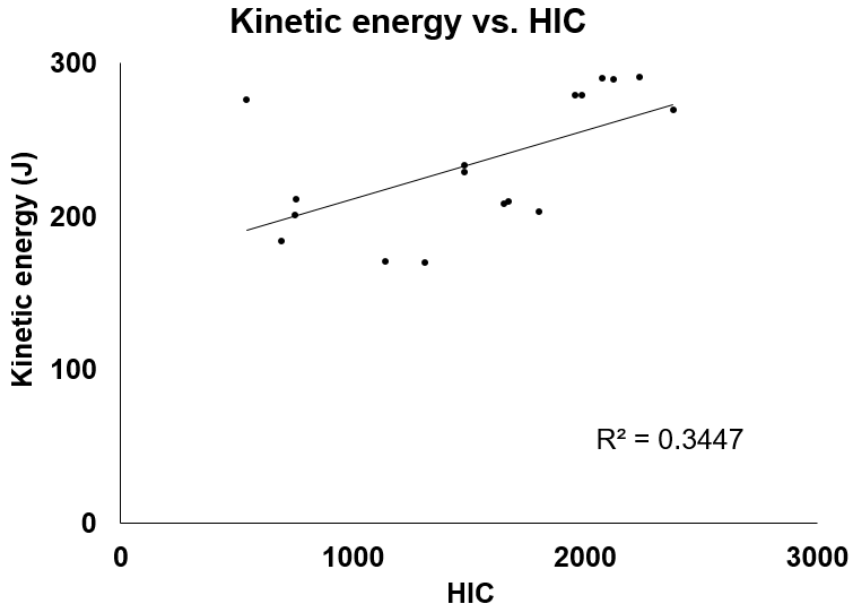

Figure 26 The correlation between kinetic energy and HIC.

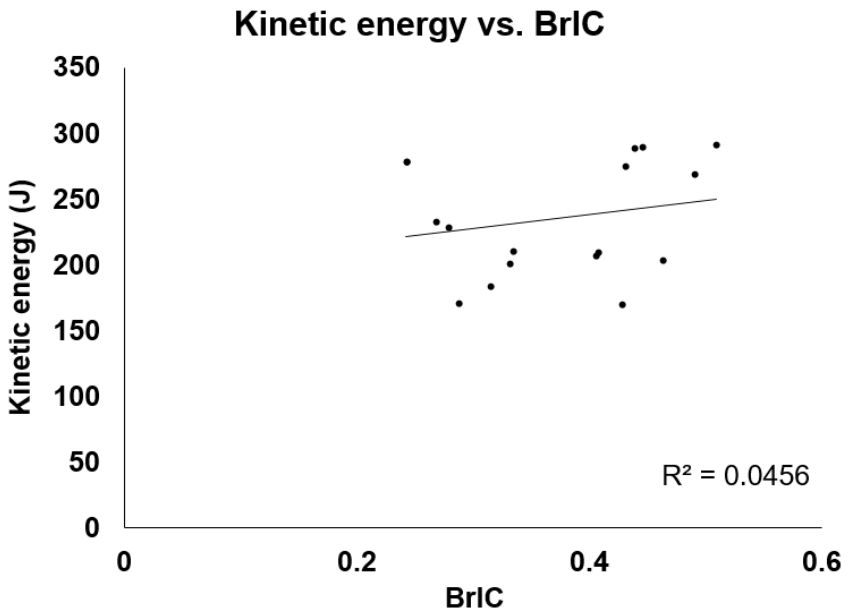

Figure 27 The correlation between kinetic energy and BrIC

Conclusions and recommendation of injury criteria

In the following section, we provide preliminary recommendation on injury criteria based on the collected data.

HIC

HIC15 was recommended as it could help mitigate stress-related skull fractures. Due to the nature of short-impact durations of sRPAS to head impacts (**Figure 5**), HIC15 would be sufficient to capture maximum HIC values. Also, using HIC10 or HIC5 would be unnecessary.

BrIC

Further investigation on BrIC is still needed. Specifically, how BrIC, or a new injury metric, could better correlate to brain strain needs to be studied. It also remains interesting that BrIC worked better to correlate with brains strains for small female but was not as good in average male cases based on current data. More impact cases and analysis are needed to further investigate the differences observed between average male and small female.

HIC affected by sRPAS structure

Due to sRPAS structural variances, how and where the sRPAS interacts with the head would greatly affect HIC values. From this point of view, simple blocks could be used to minimize the effects of structural variances. The limitation and benefit for such a simple block need to be further investigated.

Peak linear acceleration

Considering the observation that peak linear acceleration being strongly correlated to HIC15, it would be redundant to regulate both peak linear acceleration and HIC15.

80 g, 3 ms clip

With short impact durations (**Figure 5**), the 80g, 3ms clip would not fit for sRPAS to human head impact safety regulation. Hence the 80 g, 3 ms clip was not further analyzed and was not recommended.

Small female

A sRPAS tested on small female dummy is expected to yield much higher HIC numbers and BrIC numbers compared to those on average male dummy. However, it remains to be further investigated as higher HIC in small female did not necessarily induce higher skull stresse, but did induce much larger brain strains.

Validation and limitation

A representative quadcopter sRPAS was developed and the impacts between the sRPAS and male heads were validated against published cadaver data. Hence, the conclusions drawn from the male model were within reasonable confidence. Meanwhile, it needs to be recognized that there were no data to validate the sRPAS to small female head impacts. It is noticed that both male and small female human body models are two human body models commonly used and accepted by the automotive safety field and were calibrated by the same developer.

It needs to be acknowledged that the conclusions derived from one specific sRPAS model could have limited the scalability of this study.

References

1. Chung LK, Cheung Y, Lagman C, Yong NA, McBride DQ, Yang I. Skull fracture with effacement of the superior sagittal sinus following drone impact: a case report. Child's nervous system. 2017;33(9):1609-11.
2. Atwater DM. The Commercial Global Drone Market. Graziadio Business Review. 2015;18(2).
3. Olivares G, Bolte J, Prabhu R, Duma S. Task A14: UAS Ground Collision Severity Evaluation. 2017-2019.

4. Takhounts EG, Craig MJ, Moorhouse K, McFadden J, Hasija V. Development of brain injury criteria (BrIC). Stapp car crash journal. 2013 Nov;57:243-66. PubMed PMID: 24435734.
5. Prasad P, Mertz HJ, Dalmotas DJ, Augenstein JS, Diggs K. Evaluation of the field relevance of several injury risk functions. Stapp car crash journal. 2010 Nov;54:49-72. PubMed PMID: 21512903.